

## OXIDATION OF PHENOL IN ACIDIC AQUEOUS SUSPENSIONS OF MANGANESE OXIDES

LJERKA UKRAINCZYK AND MURRAY B. MCBRIDE<sup>1</sup>

Department of Soil, Crop and Atmospheric Sciences, Cornell University, Ithaca, New York 14853

**Abstract**—Phenol (benzenol) oxidation by three synthetic manganese oxides (buserite, manganite, and feitknechtite) has been studied in aerated, aqueous, acidified suspensions. The rate of reaction was pH dependent. Oxidation was greatly enhanced below pH 4, when diphenoquinone and p-benzoquinone were identified as the first products. Initial reaction rate was correlated with standard reduction potential ( $E^\circ$ ) of the oxides following the order: feitknechtite > manganite > buserite. A more gradual process of phenol oxidation after the initial reaction was influenced by electrochemical properties of the solution. High soluble manganese activity and increase in pH adversely affected reaction rates. Thus, the reactivity of the oxides was related to their stability and possibly the ability to readsorb Mn(II), following the order: buserite > manganite > feitknechtite. The results indicate that thermodynamic and electrochemical data for oxides and phenols are useful in predicting under which conditions phenols can be oxidized by a given system.

**Key Words**—Buserite, Feitknechtite, Manganese oxide, Manganite, Oxidation, Phenol, Quinones, Reduction potential.

### INTRODUCTION

Manganese oxides can act as electron-transfer agents in reactions that involve phenolic compounds and molecular oxygen (Ono *et al.*, 1977; Stone and Morgan, 1984; McBride, 1987, 1989a, 1989b; Stone, 1987; Kung and McBride, 1988; Ulrich and Stone, 1989). The manganese +2, +3, and +4 oxidation states appear to be involved in electron-transfer reactions, but the factors influencing the reactions are still poorly understood.

Phenol disappearance from acidified water samples in the presence of manganese oxide has been observed by Thielemann (1971). The extent of decrease in phenol concentration was greatest at low pH. No change in phenol concentration was observed for samples at pH > 6 over a period of days. Chen *et al.* (1991) investigated low phenol recoveries by EPA Method 625 in water samples containing manganese, and found phenol was oxidized to p-benzoquinone in acidified water samples containing manganese oxides. No detailed systematic study of conditions under which phenol oxidation by manganese oxides occurs has been conducted.

This study investigated some properties of oxides (stability, structure, reduction potential, manganese oxidation state, surface area), and solutions (phenol and manganese(II) concentrations, pH, presence of complexing agent) that influence the kinetics of oxidation of unsubstituted phenol by manganese oxides.

### MATERIALS AND METHODS

Buserite in Na-saturated form ( $\text{Na}_4\text{Mn}_{14}\text{O}_{27}\cdot 9\text{H}_2\text{O}$ ) was synthesized according to the procedure of Mc-

Kenzie (1981). Solutions of 0.8 M  $\text{MnSO}_4$  in 1 liter water and 11 M NaOH in 3 liters water were cooled to 5°C and mixed. Oxygen was bubbled through the mixture for 5 hours. Buserite in Mg-saturated form was prepared by washing Na-buserite with 0.1 M  $\text{Mg}(\text{NO}_3)_2$  (Giovanoli *et al.*, 1975). This form was chosen for experiments because it is more stable than other non-transition metal buserites (Giovanoli *et al.*, 1975), and it does not collapse to the 0.7 nm phase until the relative humidity is less than 10% (Tejedor-Tejedor and Paterson, 1979). The oxide was air-dried and ground gently in a mortar. Freeze-drying was avoided because it resulted in removal of interlayer water. X-ray powder diffraction (XRD) showed characteristic d-values of 0.959, 0.479, and 0.320 nm.

Manganite ( $\gamma\text{-MnOOH}$ ) was synthesized by the method of McKenzie (1971). Manganese(II) hydroxide was precipitated by adding 1 liter of 0.75 M NaOH to 2 liters of 0.35 M  $\text{MnSO}_4\cdot\text{H}_2\text{O}$ , and washed by decantation keeping the flask stoppered. It was oxidized to a mixture of hausmannite and manganite by slowly adding 90 ml of 30% hydrogen peroxide. The mixture was boiled while bubbling with air for 35 days, at which time XRD showed d-values of manganite: 0.342, 0.264, 0.226, 0.220, 0.170, 0.167, and 0.165 nm. The infrared spectra showed strong sharp bands characteristic of manganite at 1087, 1119 and 1149  $\text{cm}^{-1}$ . The oxide was washed and sonicated repeatedly with distilled water to remove the excess salts, and then freeze-dried.

Feitknechtite ( $\beta\text{-MnOOH}$ ) was synthesized according to the method of Hem *et al.* (1982) by raising the pH of 900 ml of 0.0098 M  $\text{Mn}(\text{ClO}_4)_2$  to 9.00, and holding it at that pH by addition of carbonate-free 0.2 M NaOH until the reaction was complete. The temperature of the solution was held between 0° and 2°C

<sup>1</sup> Corresponding author.

Table 1. Properties of manganese oxides.

Oxide	Average Mn oxidation state	% Mn	Formula	E°(V)
Mg-buserite	3.55	44	MgMn <sub>10</sub> O <sub>18.7</sub>	1.25 <sup>1,2</sup>
Manganite	3.01	60	MnO <sub>1.5</sub>	1.50 <sup>1</sup>
Feitknechtite	3.02	57	MnO <sub>1.5</sub>	1.65 <sup>3</sup>

<sup>1</sup> Bricker (1965).

<sup>2</sup> Value for birnessite is reported, since no value for buserite was available.

<sup>3</sup> Hem *et al.* (1982).

using an ice bath and air was continuously bubbled through the stirred solution. The pH was then adjusted to 4.2 with HClO<sub>4</sub> and soluble Mn<sup>2+</sup> to 168 mg/liter using a Mn(ClO<sub>4</sub>)<sub>2</sub> solution, and the suspension was stored in a refrigerator at 5°C. Following 4 days of aging, the oxide was separated from the suspension, washed, and sonicated several times with deionized distilled water, and freeze-dried. Powder XRD showed the oxide to be feitknechtite with d-spacings of 0.463, 0.253, 0.235, and 0.196 nm.

The oxidation state of Mn (Table 1) was determined by dissolving the oxide in a ferrous sulfate/sulfuric acid mixture and back-titrating a fraction of the solution with potassium dichromate in the presence of diphenylaminosulfonic acid as indicator. Another fraction of the solution was used for determining dissolved Mn by atomic absorption spectroscopy (AAS). This procedure avoids any need for drying the solid (Hem *et al.*, 1982). Dichromate titration was found superior to the commonly used permanganate titration, giving a much sharper end point, and reproducible results using commercial MnO<sub>2</sub> as a standard.

The surface area of oxides measured by BET analysis of N<sub>2</sub> adsorption was 30 m<sup>2</sup>/g for Mg-buserite, 8.5 m<sup>2</sup>/g for manganite, and 100 m<sup>2</sup>/g for feitknechtite. These values are probably lower than actual particle surface area in aqueous solution due to aggregation and sedimentation during drying (Stone, 1987). For buserite this value almost certainly corresponds only to external surface area, and does not measure the interlayer surface. A low BET surface area of manganite can be attributed to its needle-like particles collapsing together upon drying. Qualitatively, it was observed that manganite disperses into very fine particles in aqueous solutions, so it is likely to have a much larger surface area in suspension.

In oxidation experiments, a weighed quantity of oxide was combined with water and the desired amount of acid (HCl, HNO<sub>3</sub>, or CH<sub>3</sub>COOH) for 15 minutes (unless otherwise indicated) in ground-glass stoppered Erlenmeyer flasks prior to phenol addition. The mixture was stirred with a magnetic stirrer at 22° ± 1°C. Aliquots of suspension were withdrawn during reaction and filtered through 0.2 μm Nucleopore membrane

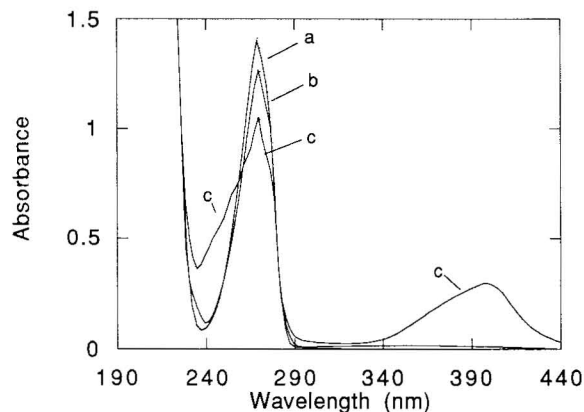


Figure 1. Phenol disappearance from solution in the presence of Mg-buserite: (a) phenol absorption (269 nm) before reacting with Mg-buserite, (b) phenol absorption after reaction with Mg-buserite when no acid was added (pH 6.05), (c) phenol absorption after reaction with Mg-buserite when acid was added ( $4 \times 10^{-3}$  M HCl, pH 3.01). Note the new peaks appearing at 398, 253, and 245 nm. Starting reaction conditions: 2g/liter Mg-buserite,  $10^{-3}$  M phenol. Reaction time is 90 seconds.

filters. The filtrate was immediately scanned by UV-VIS spectrometry (Perkin-Elmer Lambda 4C spectrometer). The phenol concentration was obtained from absorption intensity at 269 nm. Baseline adjustment was applied to the calculation of concentration to eliminate the interfering absorbance of products in solution. The pH measurements were made on a Fisher Model 805 research pH meter with a combination electrode.

Dissolved Mn<sup>2+</sup> was not measured in filtrates by AAS because preliminary experiments showed that colloidal manganese oxide particles would occasionally pass through the filter membrane causing great fluctuations in measurements. Instead, Mn<sup>2+</sup> was monitored in parallel experiments by an electron spin resonance (ESR) spectrometer (Varian E-104) at X-band frequency. The reacting suspension was continuously circulated by the Masterflex peristaltic pump through a flat, flow-type ESR cell. Relative Mn<sup>2+</sup> signal amplitudes were converted to concentrations using aqueous MnSO<sub>4</sub> standards. It was assumed that adsorbed Mn<sup>2+</sup> does not contribute to an ESR signal due to relaxation effects.

For chromatographic separation of products, the filtered reaction suspension was extracted by dry ethyl ether. Analysis of the products was performed by gas chromatography-Fourier transform infrared spectroscopy-mass spectroscopy (GC/IR/MS). The GC used was a Hewlett-Packard 5890, Series II with a 25 m HP-17 capillary column (0.32 mm ID, coating thickness of 0.52 μm), and temperature-programmed from 60° to 260°C at 8°C/min. The mass spectral detector (Hewlett-Packard 5970) was set to acquire scans over a range of m/z 40 to 550.

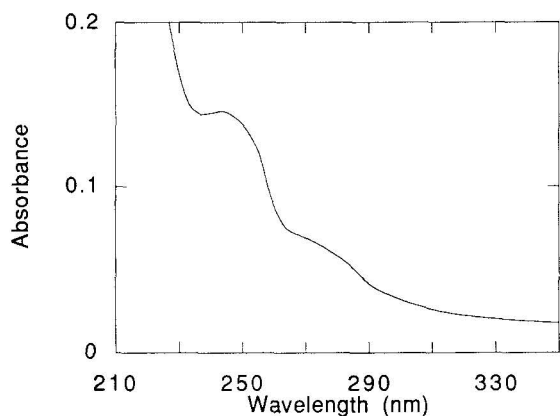


Figure 2. UV spectrum of filtered solution after all phenol has been oxidized. Starting reaction conditions: 0.5 g/liter Mg-buserite,  $10^{-4}$  M phenol,  $3.3 \times 10^{-4}$  M  $\text{HNO}_3$ , pH 2.78. Reaction time is 3 hours, pH 3.20.

## RESULTS

### Spectroscopic studies

A reaction between phenol and acidified buserite, manganite or feitknechtite suspensions produces yellow-colored solutions. Absorption spectra of the filtrate exhibit a strong peak at 398 nm, and an upward shift of baseline with weaker peaks between 240 and 265 nm (Figure 1). The peaks at 398 nm ( $\epsilon = 69,000$ ) and weak peaks at 263 nm ( $\epsilon = 2350$ ), and 253 nm ( $\epsilon = 2500$ ) are characteristic of diphenoquinone (DPQ) (Brown and Todd, 1954). The absorption band of phenol at  $\lambda_{\text{max}}$  (269 nm) loses intensity, and eventually disappears if the pH is kept below 4 in the presence of excess manganese oxide (Figure 2). After the phenol absorbance band is gone an absorption spectrum with maximum at 245 nm, typical for p-benzoquinone, remains. The same quantity of phenol solution added to

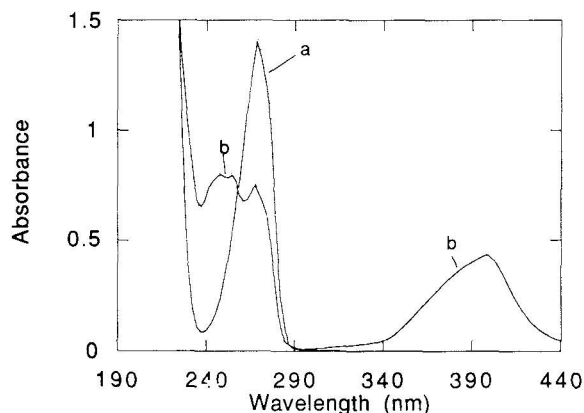


Figure 3. Phenol oxidation at higher oxide concentration: (a) UV-VIS spectrum of  $10^{-3}$  M phenol before reaction, and (b) after 30 minutes of reaction (pH 4.91). Starting reaction conditions: 4g/liter Mg-buserite,  $10^{-2}$  M HCl, pH 2.95.

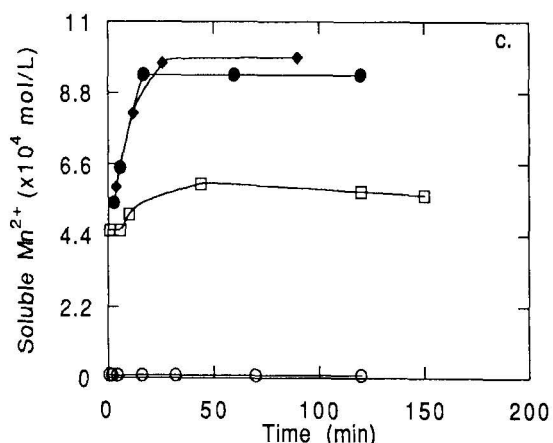
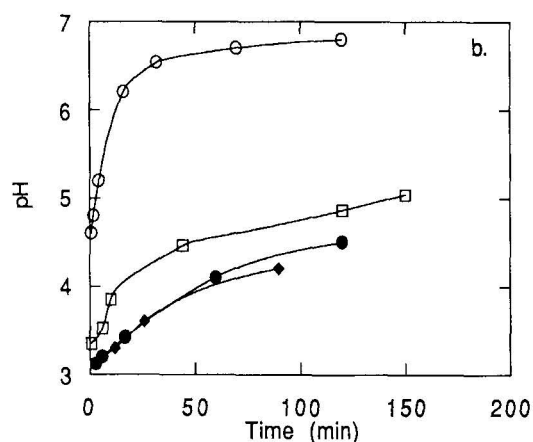
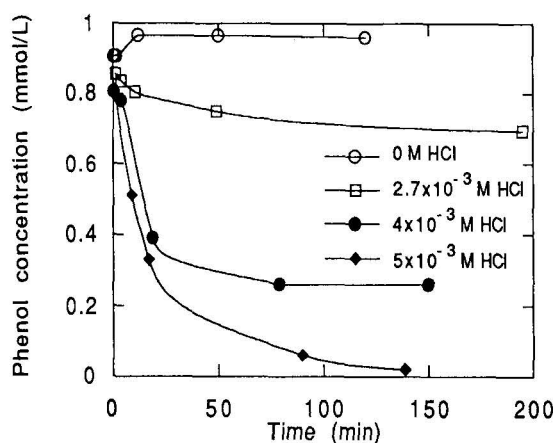


Figure 4. Change in: (a) phenol concentration, (b) pH, and (c)  $\text{Mn}^{2+}$  concentration in solution, as a function of time for different levels of acid added. Starting reaction conditions: 0.5 g/liter Mg-buserite,  $10^{-3}$  M phenol.

larger quantities of oxide suspension results in stronger absorption at 245 nm (Figure 3). The yellow-colored product is evidently unstable, building up initially and then diminishing. Both suspension and filtered solu-

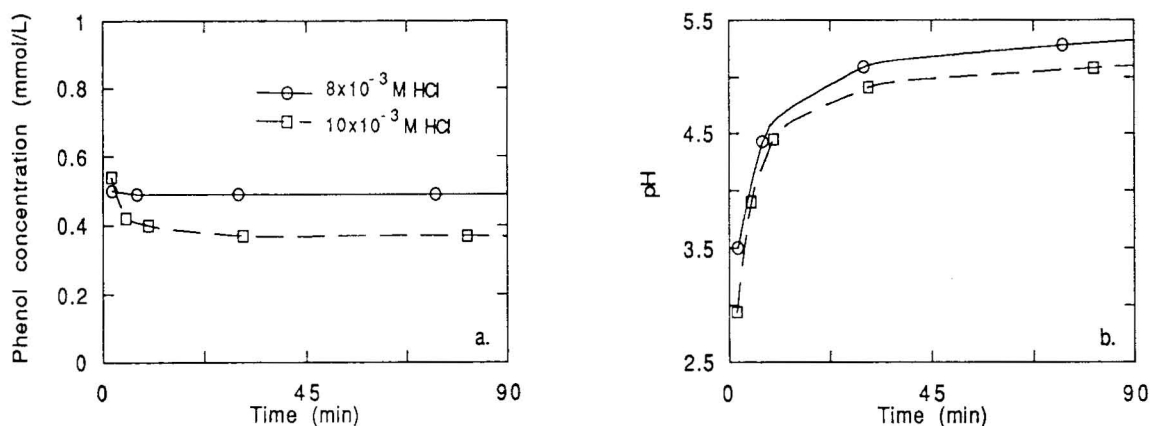


Figure 5. Change in: (a) phenol concentration, and (b) pH, as a function of time at high oxide : phenol ratio. Starting reaction conditions: 4 g/liter Mg-buserite,  $10^{-3}$  M phenol.

tion turn colorless over a period of hours or days depending on phenol concentration, product concentrations, and pH. This transformation was not investigated in detail since reactions longer than three hours could conceivably have had significant microbial contribution to organic transformations.

When the manganese oxide suspension was adjusted above pH 4 no absorption peak at 398 nm appeared, and very little reduction in the phenol absorption band occurred.

The ether extract of filtered reacting suspension is yellow-colored. An analysis by GC/IR/MS of the extract from filtered suspension in which all phenol has been oxidized revealed three products of high mass-to-charge ratio,  $m/z$  ( $m/z = 346, 390, 390$ ). Their gas phase FTIR spectra had bands at  $1730 \text{ cm}^{-1}$  and  $1642 \text{ cm}^{-1}$ , characteristic for C=O and C=C stretching, respectively.

#### Kinetic studies

Changes in phenol concentration with time at different levels of acid added ( $0, 2.7 \times 10^{-3}, 4 \times 10^{-3}$  and  $5 \times 10^{-3}$  M HCl) are shown in Figure 4 for reaction between 0.5 g/liter Mg-buserite and  $10^{-3}$  M phenol. With no acid, or small amounts of acid added, phenol concentration in the filtrate is typically lowered in the first few minutes of the experiment, and then it increases until it approaches the initial concentration. This pattern of initial decrease followed by an increase in phenol concentration at  $\text{pH} > 4$  is observed for Mg-buserite, but not for manganite and feitknechtite, for which only a slight reduction in phenol concentration is observed. It could be that upon mixing, Mg-buserite promotes phenol dissociation and adsorption by ligand exchange, lowering the pH. Phenolate (weak ligand) is then subsequently replaced by hydroxyl generated from a secondary reaction having slower kinetics. This hydroxyl may arise from proton adsorption on the oxide,

effectively raising the activity of  $\text{Mg}^{2+}$  and  $\text{OH}^-$  in solution.

If the initial pH is adjusted below 4, phenol concentration in suspension decreases as the pH of the acidified oxide suspension increases (Figure 4b), and as  $\text{Mn}^{2+}$  is released into solution (Figure 4c).

Initial rates (time less than 1 minute) of phenol oxidation mostly depend on the following conditions at the start of reaction: (1) oxide : phenol ratio, (2) pH and soluble manganese, and (3) reduction potential of the particular oxide. The effects of these conditions are: (1) high oxide : phenol ratio results in fast initial rates of phenol oxidation (compare Figures 5a and 6a), (2) low pH at the start of the reaction increased initial rates of phenol disappearance. Figure 7a illustrates the effect of pH and soluble manganese at the beginning of the reaction on the decrease in phenol concentration with time. These differences in pH and  $\text{Mn}^{2+}$  were achieved by equilibrating equally acidified aqueous oxide suspensions for different time periods (0, 0.5, and 24 hours) prior to reacting with phenol. Longer equilibration time results in higher pH and soluble manganese at the start of reaction with phenol, so less phenol is oxidized, and (3) oxides with higher standard redox potentials oxidize more phenol initially (on a weight basis). The order of initial phenol oxidation rates was feitknechtite > manganite > buserite (Figures 6a, 6b, and 9a), consistent with reported reduction potentials for these oxides (Table 1).

The more gradual phenol oxidation after the initial reaction depends on three factors influencing the redox potential of the solution: (1) pH, (2) oxide stability, dissolution and resultant effects on  $\text{Mn}^{2+}$  activity, and (3) initial phenol concentration. The three effects of these factors are: (1) Rate depends on pH as shown by suspensions buffered below pH 4 (Figure 8). Low pH resulted in a faster rate of phenol oxidation. In unbuffered suspensions, the increase in pH during phenol

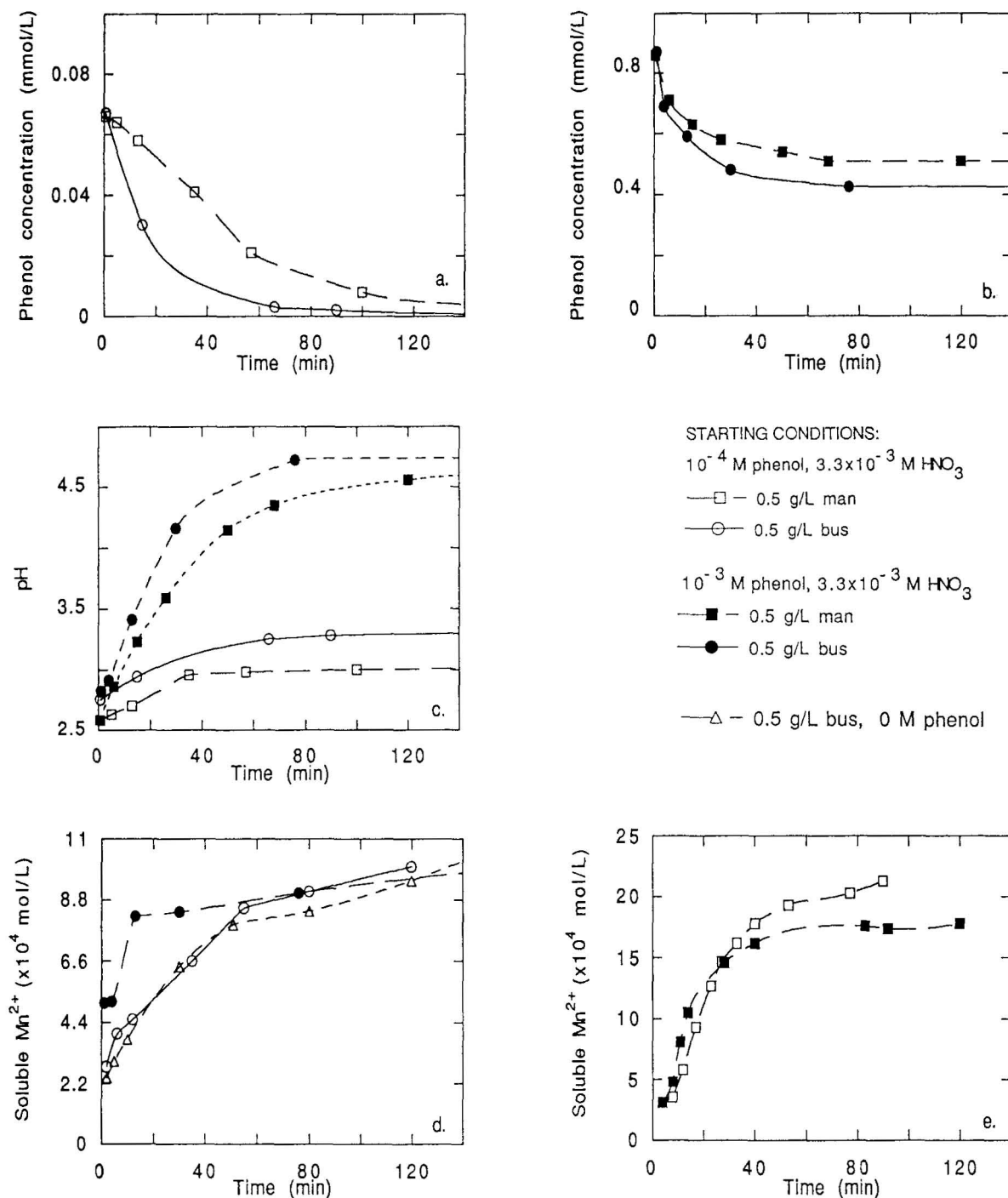


Figure 6. Change in: (a, b) phenol concentration, (c) pH, and (d, e)  $\text{Mn}^{2+}$  in solution, as a function of time for busenite and managanite at two different phenol concentrations.

oxidation plays a major role in diminishing the subsequent oxidation rate. In acetate-buffered suspensions the oxidation of phenols tends to proceed at a more nearly constant rate until much of the phenol has been oxidized. A rapid pH increase during the fast initial

reaction with large quantities of oxide (4 g Mg-busenite/liter) results in no detectable change in phenol concentration after the initial reaction (Figure 5). Here quinone build-up in solution could also suppress the longer term oxidation rate. (2) Oxide stability decreases

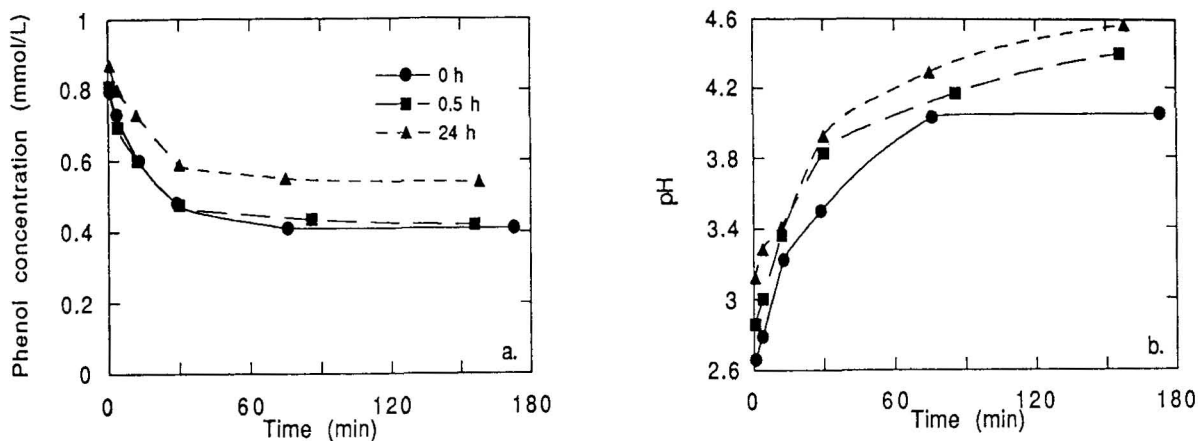


Figure 7. Change in: (a) phenol concentration, and (b) pH, as a function of time for different pH and soluble  $Mn^{2+}$  at the beginning of reaction. Suspensions were equilibrated for different time periods with the acid prior to phenol addition. Starting reaction conditions: 0.5 g/liter Mg-buserite,  $10^{-3}$  M phenol,  $3.3 \times 10^{-3}$  M HCl, (●)  $2.4 \times 10^{-4}$  M, (■)  $5.3 \times 10^{-4}$  M, and (▲)  $11.1 \times 10^{-4}$  M  $Mn^{2+}$ .

in the same order as its ability to oxidize phenol at the slow rate: buserite > manganite > feitknechtite (Figure 9). Feitknechtite and manganite are unstable at low pH (Bricker, 1965; Hem *et al.*, 1982). They "leak" large quantities of  $Mn^{2+}$  into solution generating high soluble manganese concentration. High soluble  $Mn^{2+}$  activity inhibits phenol oxidation, as was shown by reacting phenol with oxide, with and without  $2 \times 10^{-3}$  M  $MnCl_2$  added to solution (results not shown). The inhibition could be the result of lowering the oxidation potential of the system. High reduced manganese could also poison the surface by sorption (for example, via  $H^+$ - $Mn^{2+}$  exchange), or by preventing the diffusion of reduced manganese from the surface into solution. However, if the activity of soluble manganese is lowered by the

presence of a complexing agent, such as acetate, there is still considerable oxidation even at high soluble manganese concentration (Figure 8). (3) Initial phenol concentrations affect changes in pH and, hence, in the long-term reaction rates in unbuffered suspensions. At low initial phenol concentration ( $10^{-4}$  M), pH remains low and most phenol not oxidized initially is oxidized by the slow reaction (Figures 6a, 6c). Conversely, at higher phenol concentration ( $10^{-3}$  M), suspension pH rises quickly which slows the reaction (Figures 6b, 6c). This increase in pH could explain similar amounts of  $Mn^{2+}$  dissolved (although at different rates), with and without phenol present in unbuffered suspensions (Figure 6d), as opposed to a large difference in dissolved  $Mn^{2+}$  for acetate-buffered suspensions with and without phenol

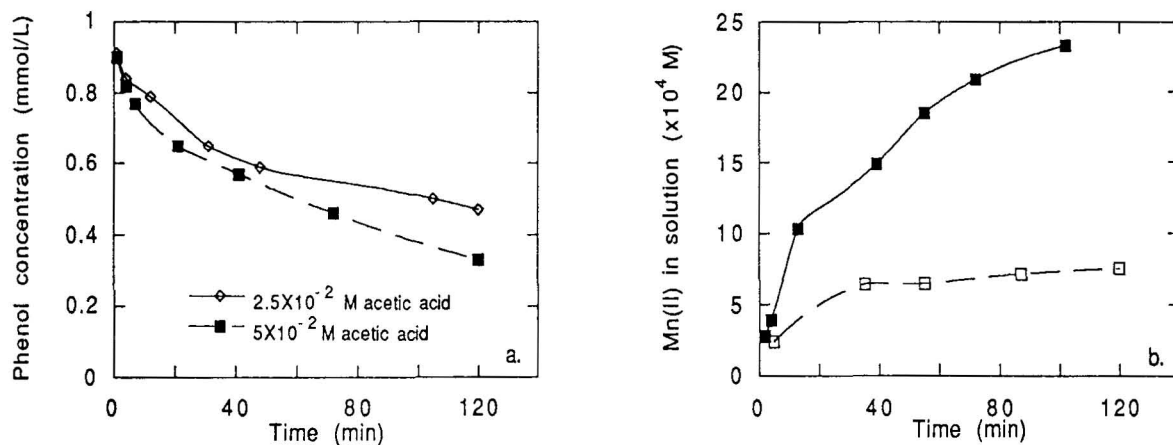
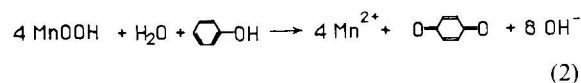
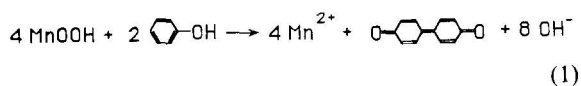


Figure 8. (a) Change in phenol concentration as a function of time for acetate buffered suspensions: (◇) pH 3.75, and (■) pH 3.50. Starting reaction conditions: 0.5 g/liter Mg-buserite,  $10^{-3}$  M phenol. (b) Dissolution of oxide with time in the presence of  $5 \times 10^{-2}$  M acetic acid, with (■) and without (□) phenol.

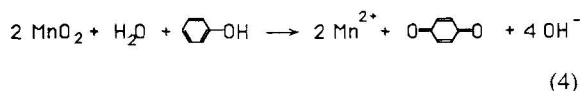
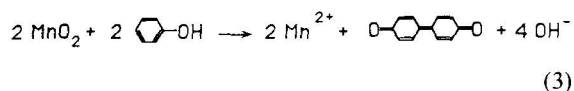
(Figure 8b). At higher pH manganese oxides can dissolve by phenol oxidation only, whereas at  $\text{pH} < 3.5$  they dissolve by oxidation of water as well.

### DISCUSSION AND CONCLUSIONS

The spectroscopic results of Figures 1–3 establish that below  $\text{pH} 4$  phenol is oxidized irreversibly by manganese oxides, possibly via two reactions (assuming a  $\text{Mn}^{3+}$ -dominated surface, Murray *et al.*, 1985):



Alternatively,  $\text{Mn}^{4+}$  may act as a two-electron acceptor:



Surface  $\text{Mn}^{3+}$  (high-spin  $d^4$ ) is expected to be Jahn-Teller distorted and, hence, kinetically labile to substitution. Thus, the gain of an electron by  $\text{Mn}^{3+}$  in reactions (1) and (2) is likely to proceed by direct coordination of phenolate to metal into an empty sigma orbital ( $t_{2g}^3 e_g^1 \rightarrow t_{2g}^3 e_g^2$ ) without change in spin state during electron transfer. This is much easier than an outer sphere electron transfer into a metal pi-orbital, which would require a change in spin rate.

On the contrary, oxidations by  $\text{Mn}^{4+}$  (Eqs. 3 and 4) would have to involve outer sphere electron transfer ( $t_{2g}^3 \rightarrow t_{2g}^3 e_g^2$ ) since the manganese(IV)–oxygen bond is too strong to afford the formation of an inner sphere complex between manganese and phenolate. Electron transfer would then require a change in the manganese spin state in the activated complex, making the oxidation more difficult.

Several other arguments against reactions (3) and (4) need to be considered. First, manganese(IV) has a lower reduction potential than manganese(III) (Yamaguchi and Sawyer, 1985). Second, “activated” forms of manganese oxides are known to require 4–8% of water of hydration, which implies the presence of  $\text{Mn}-\text{OH}$  (Evans, 1959). The fact that pure  $\text{MnO}_2$  (pyrolusite) is “inactive,” although it has the same crystal structure as manganite (McKenzie, 1989), further suggests the nonreactive nature of  $\text{Mn(IV)}$  in electron-transfer processes at the aqueous solution–oxide interface.

The production of DPQ (Eq. 1) seems to be predominant when the phenol concentration is high, while

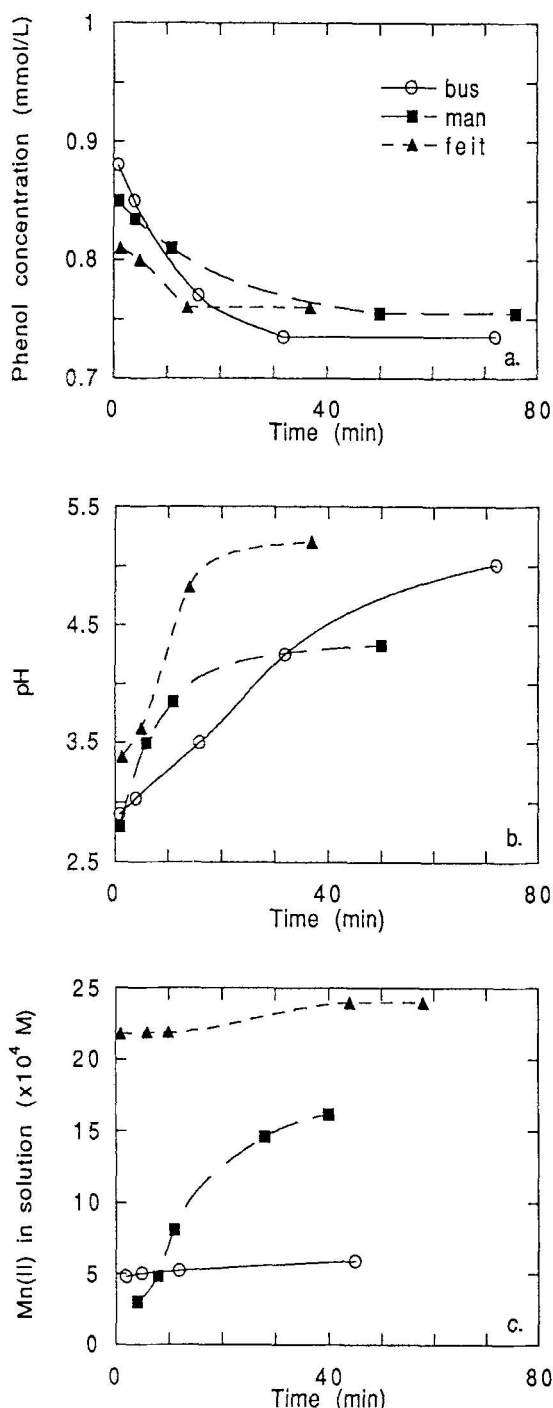


Figure 9. Change in: (a) phenol concentration, (b) pH, and (c)  $\text{Mn}^{2+}$ , as a function of time for different manganese oxides. Starting reaction conditions: 0.5 g/liter oxide,  $10^{-3}$  M phenol,  $2.7 \times 10^{-3}$  M  $\text{HNO}_3$ .

more p-benzoquinone (Eq. 2) is formed at low levels of phenol, or higher oxide concentrations. This implies that dimer formation is diffusion-controlled, requiring a higher concentration of phenol at the interface. It is

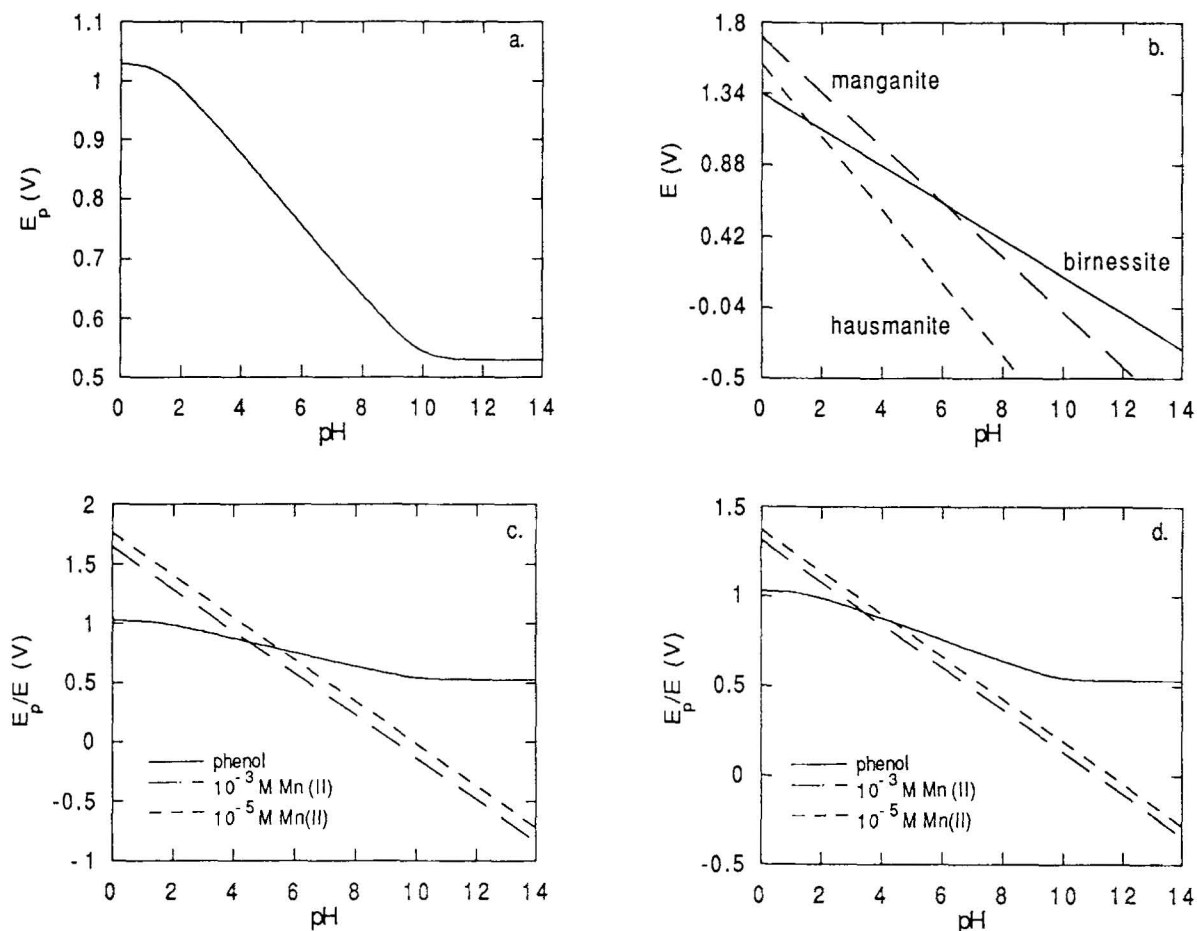


Figure 10. (a) Electrochemical peak potential (vs. std.  $H_2$  electrode) of phenol as a function of pH (determined by Wisser and Bubb, 1980; for explanation see Zuman and Holthuis, 1988). (b) Reduction potential of manganite, birnessite, and hausmanite at 25°C, as a function of pH at  $10^{-4}$  M  $Mn^{2+}$  activity (Bricker, 1965; Eqs. 22, 31, and 12, respectively). (c) Reduction potential of manganite, and electrochemical peak potential of phenol, as a function of pH. (d) Reduction potential of birnessite, and electrochemical peak potential of phenol, as a function of pH.

not known whether oxygen for benzoquinone formation comes from the oxide, dissolved  $O_2$ , or water.

Other studies of the products of phenol oxidation at low pH (Waters, 1971; McDonald and Hamilton, 1973) similarly found C-C coupling and quinone formation favored over polymer formation by C-O coupling. This is attributed to phenoxy radicals remaining complexed to the metal ion during coupling (McDonald and Hamilton, 1973). In the present study, the persistence of a surface phenoxy manganese complex after electron transfer is suggested by the failure of ESR to detect any radicals in solution (however, phenol radicals, if formed, are likely to be too short-lived to be detected by ESR). Such a complex could make the *ortho* positions on phenol sterically inaccessible, accounting for the fact that reactivity was limited to the *para* position as indicated by the oxidation products formed.

The amount of diphenoquinone formed is far less than the amount of phenol oxidized, a fact which can

be attributed to the instability of DPQ. The pathway of DPQ decomposition could not be followed by UV-VIS spectroscopy, but considering its high reduction potential (0.954 V; Brown and Todd, 1954), it could couple oxidatively with phenol, yielding phenolic and quinoid oligomers and polymers insoluble in water. This may explain the loss of the yellow color in solution with time. At least some of the high molecular weight products were soluble in ethyl ether since they were detected by GC/IR/MS.

The amount of p-benzoquinone formed is also very small. Chen *et al.* (1991) explained a similar observation in terms of the formation of oxidation products that were either insoluble in acidic media, or undetectable by the method used for analysis (GC/MS).

The effect of pH in redox processes is of great importance in changing the thermodynamic potentials and the kinetics of electron transfer. The thermodynamic redox potential for phenol cannot be measured



since its oxidations are irreversible. Instead, electrochemical peak and half potentials ( $E_p$  and  $E_{1/2}$ ) obtained by polarography are used. The plot of  $E_p$  vs. pH for the oxidation of phenol (Figure 10a) indicates that  $E_p$  becomes more positive as the solution is made more acidic; i.e., phenol is more difficult to oxidize at low pH. Conversely, manganese oxides become more effective oxidants as pH is decreased (Figure 10b). If the manganite and birnessite stability lines at two arbitrarily chosen  $Mn^{2+}$  activities ( $10^{-3}$  and  $10^{-5}$  M) are superimposed on the phenol curve (Figures 10d, 10e), the pH range within which it is thermodynamically possible to oxidize phenol by these oxides is indicated. According to Eqs. (1) and (2), phenol concentration and product concentration are also important in determining the magnitude and the sign of the reaction affinity. High soluble  $Mn^{2+}$  activity could make reactions less favorable. Below pH 3.5 manganese oxide also dissolves by oxidation of water. Consequently, the amount of  $Mn^{2+}$  produced is higher than expected from phenol oxidation. Buserite is known to have a high preference for  $Mn^{2+}$ , which can selectively exchange other interlayer cations. This would tend to maintain a low  $Mn^{2+}$  activity in solution. When acetate is present, the oxide dissolution is further facilitated by complexation, but the activity of manganese in solution is likely to be much lower than the actual concentration, making the reduction potential of the system more positive. Manganese complexation by acetate could also facilitate the removal of reduced manganese from the solution-oxide interface, thus exposing "clean" reactive surfaces. In open systems, the removal of  $Mn^{2+}$  and oxidation products by leaching would be expected to maintain reaction conditions more favorable than those in the closed systems of this study.

#### SIGNIFICANCE

The oxidation of various substituted phenols by manganese oxides has been previously studied (Stone, 1987; Ulrich and Stone, 1989), and a similar pH dependence of reaction rates has been observed. Electrochemical half- or peak-potential depends on kind, number, and position of substituents on the aromatic ring (Suatoni *et al.*, 1961). It has been shown that there is a linear relationship between  $E_p$  and the Hammett constant of substituents, and between  $E_p$  and ionization potential of the molecule. The  $E_p$  of substituted phenols shows similar dependence on pH as that for unsubstituted phenol (Ronlan, 1978, and references therein). Thus the  $E_p$ -vs.-pH relationship can be used to predict under which conditions the oxidation of a certain phenol is thermodynamically plausible.

#### REFERENCES

Bricker, O. (1965) Some stability relations in the system  $Mn-O_2-H_2O$  at 25° and one atmosphere total pressure: *Amer. Mineral.* **50**, 1296–1354.

- Brown, B. R. and Todd, A. R. (1954) Colouring matters of the *Aphididae*. Part IX. Some reactions of extended quinones: *J. Chem. Soc.*, 107–110.
- Chen, P. H., VanAusdale, W. A., and Roberts, D. F. (1991) Oxidation of phenolic acid surrogates and target analytes during acid extraction of natural water samples for analysis by GC/MS using EPA Method 625: *Environ. Sci. Technol.* **25**, 540–546.
- Evans, R. M. (1959) Oxidations by manganese dioxide in neutral media: *Quart. Rev. Chem. Soc.* **13**, 61–70.
- Giovanoli, R., Burki, P., Giuffredi, M., and Stumm, W. (1975) Layer structured manganese oxide hydroxides. IV: The buserite group; structure stabilization by transition elements: *Chimia* **9**, 517–520.
- Hem, J. D., Roberson, C. E., and Fournier, R. B. (1982) Stability of  $\beta MnOOH$  and manganese oxide deposition from springwater: *Water Resour. Res.* **18**, 563–570.
- Kung, K.-H., and McBride, M. B. (1988) Electron transfer between hydroquinone and hausmannite ( $Mn_3O_4$ ): *Clays & Clay Minerals* **36**, 503–509.
- McBride, M. B. (1987) Absorption and oxidation of phenolic compounds by iron and manganese oxides: *Soil Sci. Soc. Am. J.* **51**, 1466–1472.
- McBride, M. B. (1989a) Oxidation of dihydroxybenzenes in aerated aqueous suspensions of birnessite: *Clays & Clay Minerals* **37**, 341–347.
- McBride, M. B. (1989b) Oxidation of dihydroxybenzenes by birnessite in acidic buffered solutions: *Clays & Clay Minerals* **37**, 479–486.
- McDonald, P. D. and Hamilton, G. A. (1973) Mechanisms of phenolic oxidative coupling: in *Oxidation in Organic Chemistry, Part B*, W. S. Trahanovsky, ed., Academic Press, New York, 97–134.
- McKenzie, R. M. (1971) The synthesis of birnessite, cryptomelane, and some other oxides and hydroxides of manganese: *Miner. Mag.* **38**, 493–502.
- McKenzie, R. M. (1981) The surface charge on manganese dioxides: *Aust. J. Soil Res.* **19**, 41–50.
- McKenzie, R. M. (1989) Manganese oxides and hydroxides: in *Minerals in Soil Environments*, J. B. Dixon and S. B. Weed, eds., Soil Science Society of America, Madison, Wisconsin, 439–465.
- Murray, J. W., Dillard, J. G., Giovanoli, R., Moers, H., and Stumm, W. (1985) Oxidation of Mn(II): Initial mineralogy, oxidation state and ageing: *Geochim. Cosmochim. Acta* **49**, 463–470.
- Ono, Y., Matsumura, T., and Fukuzumi, S. (1977) Electron spin resonance studies on the mechanism of the formation of p-benzosemiquinone anion over manganese dioxide: *J. Chem. Soc. Perkin II*, 1421–1424.
- Ronlan, A. (1978) Phenols: in *Encyclopedia of Electrochemistry of the Elements, Vol. XI*, A. J. Bard and H. Lund, eds., Dekker, New York, 242–275.
- Stone, A. T. (1987) Reductive dissolution of manganese(III/IV) oxides by substituted phenols: *Environ. Sci. Technol.* **21**, 979–988.
- Stone, A. T. and Morgan, J. J. (1984) Reduction and dissolution of manganese(III) and manganese(IV) oxides by organics. 2. Survey of the reactivity of organics: *Environ. Sci. Technol.* **18**, 617–624.
- Suatoni, J. C., Snyder, R. E., and Clark, R. O. (1961) Voltametric studies of phenol and aniline ring substitution: *Anal. Chem.* **33**, 1894–1897.
- Tejedor-Tejedor, M. L. and Paterson, E. (1979) Reversibility of lattice collapse in synthetic buserite: in *Proc. Int. Clay Conf.*, M. M. Mortland and V. C. Farmer, eds., Elsevier, Amsterdam, 501–508.
- Thielemann, H. (1971) Analytische Untersuchungen über

- den katalytischen Einfluss von Mangan(IV)-oxid auf phenolhaltige Testlösungen: *Mikrochim. Acta*, 38–39.
- Ulrich, H.-J. and Stone, A. T. (1989) Oxidation of chlorophenols adsorbed to manganese oxide surfaces: *Environ. Sci. Technol.* **23**, 421–428.
- Waters, W. A. (1971) Comments on the mechanism of one-electron oxidation of phenols: A fresh interpretation of oxidative coupling reactions of plant phenols: *J. Chem. Soc. (B)*, 2026–2029.
- Wisser, K., and Bubb, F. P. (1980) Anodische Oxydation und Hydroxylierung von Monophenolen an der "mikro-rauhen" Glaskohle-Elektrode: *Mikrochim. Acta II*, 145–157.
- Yamaguchi, K. S. and Sawyer, D. T. (1985) The redox chemistry of manganese(III) and (IV) complexes: *Isr. J. Chem.* **25**, 164–176.
- Zuman, P. and Holthuis, J. J. M. (1988) Mechanism of electrooxidation of substituted phenols in aqueous solutions: some podophyllotoxin derivatives as models: *Recl. Trav. Chim. Phys-Bas* **107**, 403–406.

(Received 31 July 1991; accepted 25 November 1991; Ms. 2126)